

# Rotation Invariant Non-rigid Shape Matching in Cluttered Scenes

Wei Lian<sup>1</sup> and Lei Zhang<sup>2\*</sup>

<sup>1</sup> Dept. of Computer Science, Changzhi University, Changzhi, 046011, Shanxi, China,  
lianwei3@gmail.com

<sup>2</sup> Biometric Research Center, Dept. of Computing, The Hong Kong Polytechnic  
University, Hong Kong, cslzhang@comp.polyu.edu.hk

**Abstract.** This paper presents a novel and efficient method for locating deformable shapes in cluttered scenes. The shapes to be detected may undergo arbitrary translational and rotational changes, and they can be non-rigidly deformed, occluded and corrupted by clutters. All these problems make the accurate and robust shape matching very difficult. By using a new shape representation, which involves a powerful feature descriptor, the proposed method can overcome the above difficulties successfully, and it possesses the property of global optimality. The experiments on both synthetic and real data validated that the proposed algorithm is robust to various types of disturbances. It can robustly detect the desired shapes in complex and highly cluttered scenes.

## 1 Introduction

Point matching is a fundamental yet challenging problem in computer vision, pattern recognition and medical image analysis, while non-rigid point matching is particularly difficult due to the large number of possible non-rigid transformations of the template [1]. In this paper, we will address the following problem under the non-rigid point matching framework: locating a deformable shape in cluttered scenes. The shape may undergo arbitrary translational and rotational changes, and it may be non-rigidly deformed, occluded and corrupted by random or structured outliers. All these difficulties make shape matching a formidable task. To overcome these problems, different methods have been proposed [2], which can be classified as those based on local search and those based on global search.

**Methods based on local search.** The iterated closest point (ICP) method [3, 4] uses the closest points as the matched points, and it has variants [5, 6]. The robust point matching (RPM) method [1] uses deterministic annealing [7] to recover a continuously relaxed point correspondence. The method in [8] uses constraint projection based on quadratic programming to gradually recover the point correspondence and uses clustering for speedup. The covariance driven correspondence (CDC) method [9] uses the covariance of the transformation

---

\* corresponding author

parameters to prune the possible false point correspondences. The methods in [10, 11] convert point set registration to an image registration problem. These local search methods are generally not rotation invariant and not robust to strong outlier disturbances.

**Methods based on global search.** These methods can be further classified as those based on spatial mapping and those based on point correspondence. For the first category, solution space searching techniques such as genetic algorithm [12], particle filtering [13] and particle swarm optimization [14] can be used to recover the transformation. These methods need no initial coarse alignment and are robust against clutter, but they require an explicit modeling of the transformation and may become computationally expensive when the number of transformation parameters becomes high, which makes them unsuitable for non-rigid matching. The method in [15] constructs a global convex approximation to the matching function and thus the transformations can be optimally recovered. But the number of constraints for the method is usually very high which is circumvented by using interior point methods.

For the second category, linear programming was employed in [16, 17] to minimize both the feature matching cost and geometric distortion. Ant colony optimization was employed in [18] for contour correspondence. Dynamic programming (DP) was used to match chain-like or tree-like structures in [19, 20]. In [21], it was extended to match regions of a shape. Belief propagation was used in [22] to match shapes where shapes with loops or holes are allowed.

Shape context (SC) [23] is a very informative feature descriptor. The SC of a point is a measure of the distribution of other points relative to it. SC is very discriminative and quite robust to various types of disturbances, which makes it especially useful for non-rigid point matching. However, SC is rotation variant in most applications (i.e. no significant rotations are allowed between two point sets). Attempts at making SC rotation invariant are either susceptible to noise, tend to degrade the discriminative power of SC (e.g. tangent directions were used to determine the orientations of SCs in [23], distance between two SCs was rendered rotation invariant by traversing all rotated versions of one of them and retaining the minimum distance in [17]) or imposing unnatural requirements on point sets (e.g. the directions pointed at the mass center of a point set were used as the orientations of SCs in [24]).

We propose in this paper a new approach to representing shapes and apply it to rotation invariant non-rigid point matching. A shape is triangulated such that the non-boundary edges are long enough and also DP can be used to find the best embedding of the triangles in target point set. Then SC features are constructed for vertices of the triangles whose orientations coincide with the directions of non-boundary edges. The SC features constructed in this way are therefore rotation invariant. To further improve our method's robustness to outliers, we modify the original SC distance measure in [23] such that the SC input belonging to the template is used as a mask to reduce the influence of outliers on the SC input belonging to the target.

Compared with previous attempts at enabling SC rotation invariant, our approach retains the discriminative power of SC, is robust to orientation disturbances and appears natural. It shares similarities with the method in [21] in that both approaches use triangulation to represent shapes and DP is used to find the best embedding of triangles in target set. However, the method in [21] is for deformable template matching in images, and the purpose of triangulation is to introduce non-rigid deformation in template (constrained Delaunay triangulation is adopted to achieve the maximum effect). In comparison, the purpose of triangulation in our method is to render SC rotation invariant, where a different triangulation approach is adopted with the aim that the orientations of SCs should be as robust to disturbances as possible.

The remaining of the paper is organized as follows. Section 2 introduces briefly the shape representation. Section 3 presents a new SC distance measure. Section 4 presents the energy function. Section 5 summarizes the algorithm. Section 6 presents extensive experimental results and section 7 concludes the paper.

## 2 Shape representation

We restrict ourselves to the cases where the template point set can be represented as a simple polygon, which is a polygon without holes. We call the polygon the boundary of the set. For a general point set, we obtain its boundary by solving the traveling salesman problem [25]. We triangulate the template set such that: 1) its boundary edges are retained; 2) a point is chosen as the reference and the rest points are connected to it (the resulting edges will be called frame edges hereafter). This results in a fan-shaped triangulation. Fig. 1 shows two examples of such triangulation.

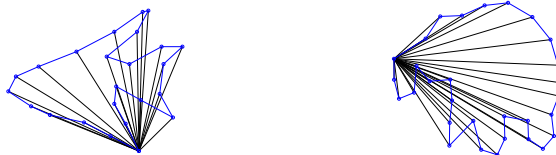


**Fig. 1.** Examples of fan-shaped triangulation. The boundaries of the shapes are highlighted in blue, and the frame edges are indicated in black.

We then compute oriented SC [23] for each point except for the reference point, whose positive x-axis is directed at the reference point. Oriented SCs constructed in this way are therefore rotation invariant. Due to the strong discriminative nature of SC, our method’s robustness to various types of disturbances is greatly enhanced.

Alternative ways of triangulation are possible, so why the fan-shaped triangulation is preferred? The orientations of SCs coincide with the directions of

frame edges in our method. We know that the longer an edge is, the less likely its orientation will be affected by positional disturbances of the endpoints. More specifically, assume the endpoints are  $x_i = \hat{x}_i + \Delta x_i, i = 1, 2$ , where  $\hat{x}_i$  denotes the noise free position and  $\Delta x_i$  denotes noise. The direction of the edge is

$$\frac{x_2 - x_1}{\|x_2 - x_1\|} \approx \frac{x_2 - x_1}{\|\hat{x}_2 - \hat{x}_1\|} = \frac{\hat{x}_2 - \hat{x}_1}{\|\hat{x}_2 - \hat{x}_1\|} + \frac{\Delta x_2 - \Delta x_1}{\|\hat{x}_2 - \hat{x}_1\|}$$

The second term comes from noise. Therefore the larger the length  $\|\hat{x}_2 - \hat{x}_1\|$  is, the less influence the noise will impose on the direction of the edge. Fan-shaped triangulation provides a simple and effective solution to ensuring that the edges determining the orientations of SC are long enough. We have also tested several alternative triangulations such as the greedy heuristic based method, where a shape is iteratively divided into two halves by choosing the longest interior edge as the splitting line, but our experimental results demonstrated that fan-shaped triangulation is more robust for point matching.

Based on the same consideration, the reference point in fan-shaped triangulation is chosen such that the average distance from it to the rest points is maximized.

### 3 Outlier resistant shape context distance

The SC of a point is defined as the distribution of other points relative to it in log-polar coordinate and is quantified as a histogram. Consider two points,  $i$  in template set and  $j$  in target set, their SCs are histograms  $h_i(k)$  and  $h'_j(k)$ , for  $k = 1, 2, \dots, K$ , respectively. The  $\chi^2$  test statistic was used to measure their difference in [23]:

$$\frac{1}{2} \sum_{k=1}^K \frac{[h_i(k) - h'_j(k)]^2}{h_i(k) + h'_j(k)} \quad (1)$$

This measure is effective when there are no outliers or the outliers are homogeneously distributed in target set. But it may become inadequate when there are structured outliers in target set.

To tackle the above problem, based on the observation that the template set is generally outlier free, let us consider the scenario where the only type of disturbance is outliers in target set. If points  $i$  in template set and  $j$  in target set correspond to each other, we would have  $h_i(k) = h'_j(k)$  for all  $k$  if there were no outliers. Since there are outliers in target set, intuitively we can use  $\text{sign}(h_i(k))$  as a mask to reduce the influence of outliers on  $h'_j(k)$ , where

$$\text{sign}(x) = \begin{cases} 1 & \text{if } x > 0 \\ 0 & \text{if } x = 0 \end{cases}$$

This is accomplished by replacing  $h'_j(k)$  with  $\hat{h}'_j(k) = \text{sign}(h_i(k)) \cdot h'_j(k)$ . We then normalize  $\hat{h}'_j$  so that it can represent a distribution:  $\sum_{k=1}^K \hat{h}'_j(k) = 1$ . We

now define the outlier resistant shape context distance (ORSCD) between two SCs  $h_i$  and  $h'_j$  as:

$$\frac{1}{2} \sum_{k=1}^K \frac{[h_i(k) - \widehat{h}'_j(k)]^2}{h_i(k) + \widehat{h}'_j(k)} \quad (2)$$

Our experimental results showed that, compared with the original SC distance measure, ORSCD's robustness to outliers is significantly improved while its robustness to non-rigid deformation is only slightly weakened.

## 4 Energy function

Fan-shaped triangulation will result in a chain of connected triangles, where two triangles are considered connected if they share a common edge, which meets the prerequisite of DP. Therefore DP can be used to find the best embedding of these triangles in target point set. In this section, we present the energy function associated with the matching problem.

Suppose that the 2D template point set is  $\mathcal{X} = \{x_i, 0 \leq i \leq n\}$ , where the sequence  $x_0, x_1, \dots, x_n, x_0$  forms its closed boundary. Without loss of generality,  $x_0$  is assumed to be the reference. Denote by  $\mathcal{Y} = \{y_j, 0 \leq j \leq m\}$  the point set to be matched. The task of matching is to find a mapping  $\phi : \mathcal{X} \rightarrow \mathcal{Y}$  which maps the  $i$ th point in  $\mathcal{X}$  to the  $l_i$ th point in  $\mathcal{Y}$  so that certain energy function can be minimized.

The energy function used in our method is

$$E(\phi) = E_{sc}(\phi) + \lambda E_{bound}(\phi) + \mu E_{frame}(\phi) \quad (3)$$

where the term  $E_{sc}$  penalizes the SC distance between the matched points, the term  $E_{bound}$  and  $E_{frame}$  require, respectively, that the lengths of boundary and frame edges should be preserved during matching. The constants  $\lambda$  and  $\mu$  ( $\lambda \geq 0, \mu \geq 0$ ) serve to balance the weights of the three terms. (We assume that the template point set is unit sized and choose  $\lambda = 1, \mu = 0.5$  in our method). For non-rigid matching, a smaller  $\mu$  allows for more non-rigid behavior of the method.

The term  $E_{sc}$  is defined as:

$$E_{sc}(\phi) = \sum_{i=1}^n D_{sc}[i, 0](l_i, l_0) \quad (4)$$

where  $D_{sc}[i, 0](l_i, l_0)$  denotes the original SC distance [23] or ORSCD between the oriented SC of  $x_i$  and the oriented SC of  $y_{l_i}$ . The positive x-axis of SC for  $x_i$  is directed at  $x_0$ , and the positive x-axis of SC for  $y_{l_i}$  is directed at  $y_{l_0}$ . The SC distances computed in this way are therefore rotation invariant.

The term  $E_{bound}$  is defined as:

$$E_{bound}(\phi) = \sum_{i=0}^{n-1} D_{bound}[i, i+1](l_i, l_{i+1}) \quad (5)$$

where  $D_{bound}[i, i+1](l_i, l_{i+1})$  denotes the length difference between the boundary edge  $(i, i+1)$  in  $\mathcal{X}$  and the candidate edge  $(l_i, l_{i+1})$  in  $\mathcal{Y}$ :

$$D_{bound}[i, i+1](l_i, l_{i+1}) = \left| \|y_{i+1} - y_i\| - \|x_{i+1} - x_i\| \right| \quad (6)$$

If the length of a boundary edge  $(i, i+1)$  in  $\mathcal{X}$  is close to 0, which often occurs in contour matching,  $D_{bound}$  can be further simplified as:

$$D_{bound}[i, i+1](l_i, l_{i+1}) = \|y_{i+1} - y_i\| \quad (7)$$

The term  $E_{frame}$  is defined as:

$$E_{frame}(\phi) = \sum_{i=2}^n D_{frame}[i, 0](l_i, l_0) \quad (8)$$

where  $D_{frame}[i, 0](l_i, l_0)$  denotes the length difference between the frame edge  $(i, 0)$  in  $\mathcal{X}$  and the candidate edge  $(l_i, l_0)$  in  $\mathcal{Y}$ . We use the  $\chi^2$  test statistic [23] instead of the Euclidean distance to measure the length difference:

$$D_{frame}[i, 0](l_i, l_0) = \frac{\left| \|y_i - y_{l_0}\| - \|x_i - x_0\| \right|^2}{\|y_i - y_{l_0}\| + \|x_i - x_0\|} \quad (9)$$

This is based on the fact that shorter edges are less distorted than longer edges under a non-rigid deformation. Therefore the length differences of shorter edges should be penalized more than those of longer edges.

## 5 Algorithm

During initialization, oriented SC is constructed for each point in  $\mathcal{X}$  with  $x_0$  serving as the reference, which has time complexity  $O(n)$  and space complexity  $O(n)$ . Oriented SC is then constructed for each point in  $\mathcal{Y}$  with all the rest points serving as possible references, which has time complexity  $O(m^2)$  and space complexity  $O(m^2)$ . Finally, distances between oriented SC features in both point sets are computed, which has time complexity  $O(nm^2)$  and space complexity  $O(nm^2)$ .

In practice, the time of computing SC features for a point in  $\mathcal{Y}$  with all the rest points serving as possible references can be reduced by quantizing orientation into  $M$  evenly distributed angles ( $M = 50$  is chosen in our method):  $0, \frac{1}{M}2\pi, \dots, \frac{M-1}{M}2\pi$ , and only computing SC features with these angles as the possible orientations. Then the SC features with all the rest points being possible references are substituted by these SC features based on orientation proximity. With this heuristic, the complexity of the initialization is essentially  $O(nm)$ .

SC distances are then used in the optimization. The algorithm is an instantiation of the well known DP technique. We compute the cost of the best placements  $l_j$  for  $j = 1, \dots, i-1$  as a function of the placements  $l_0$  and  $l_i$ , which is stored in  $V[i, 0](l_i, l_0)$ . The algorithm is summarized as follows.

Algorithm 1: Find the best embedding of a shape in a point set.
1. $V[1, 0](l_1, l_0) = D_{sc}[1, 0](l_1, l_0) + \lambda D_{bound}[0, 1](l_0, l_1)$
2. For $i = 2, \dots, n$ , do $V[i, 0](l_i, l_0) \leftarrow \min_{l_{i-1}} V[i-1, 0](l_{i-1}, l_0) + \lambda D_{bound}[i-1, i](l_{i-1}, l_i)$ ; $V[i, 0](l_i, l_0) \leftarrow V[i, 0](l_i, l_0) + D_{sc}[i, 0](l_i, l_0) + \mu D_{frame}[i, 0](l_i, l_0)$
3. Pick $l_n$ and $l_0$ minimizing $V[n, 0]$ and trace back to obtain the other optimal locations.

The above procedure has time complexity  $O(nm^3)$  and space complexity  $O(nm^2)$ . We can speed it up based on two considerations: First, if the length of a boundary edge  $(i-1, i)$  in  $\mathcal{X}$  is close to 0, given location  $l_i$ , the possible candidates for  $l_{i-1}$  should be those points near  $y_{l_i}$  [21], because points that are far from it will introduce too much distortion in the template (15 nearest points are chosen in our method). Second, given location  $l_i$ , the possible candidates for  $l_0$  should be those points which are close to the circle centered at  $y_{l_i}$  and with a radius equal to the length of the edge  $(i, 0)$  in  $\mathcal{X}$ , because points that are far from the circle will also introduce too much distortion in the template. With the two heuristics, the complexity of the proposed algorithm is essentially  $O(nm)$ .

## 6 Experimental results

We compare our method with 3 state-of-the-art methods: the local neighborhood structure preserving (LNSP) method in [24], the Viterbi algorithm (VA) based method in [26], and the linear programming (LP) based method in [16] where we choose SC as the feature descriptor. VA and LP are not rotation invariant. We render them rotation invariant by running them on 12 evenly distributed angles and retaining the result with the minimum cost. The code of our method is available at <http://www4.comp.polyu.edu.hk/~cs1zhang/code.htm>.

We implement the methods under Matlab version 7.6 on a PC with 2GHz CPU and 2G memory. We use affine transformation to model a non-rigid spatial mapping. Correspondence recovered by a method is used to solve for the affine transformation. In the following, the transformed template point set is highlighted by red \* and point correspondences are indicated by black line segments. First we use synthetic data to evaluate various aspects of the methods. Then we compare the methods using data acquired from real images.

### 6.1 Experiments using synthetic data

Synthetic data can be designed to test specific aspects of a method. First, we use the Chui-Rangarajan synthesized data sets [1] to test the methods' robustness against non-rigid **deformation**, **noise** in position and **outliers**. In each test, the template shape is subjected to one of the above distortions to create a target point set (for the latter two test sets, a moderate amount of deformation is present). Two shapes, a fish and a Chinese character, shown in the left column of Fig. 2, are used as the template shape respectively. 100 random target point sets were generated for each setting within each series. The right 3 columns of

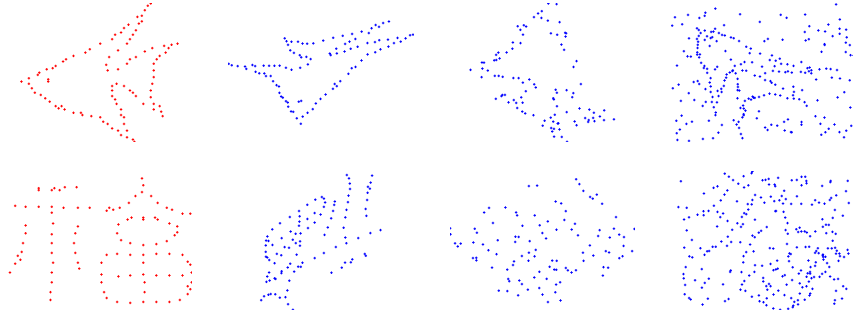


**Fig. 2.** The template point sets (left column) and examples of target point sets in the deformation, noise and outlier tests respectively (right 3 columns).

Fig. 2 show examples of target point sets in the 3 series of tests respectively. We use the original SC distance measure in our method.

The means and standard deviations of the errors of the methods are shown in Fig. 3, where error is defined as the mean of the Euclidean distances between the affinely transformed template points and their ground truth target points. It can be seen that the matching error of our method is in average compared with the other methods for the deformation and noise tests, while considerably lower than others for the outlier test. This demonstrates our method’s robustness against various types of disturbances, especially for outliers.

The average running times of the methods are listed in Table 1. It can be seen that our method’s running time is low when the number of points is low, but increases much when the number of points becomes high (i.e. in the case of outliers).

**Table 1.** Average Running Time (second)

	Deformation	Noise	Outliers
LNSP	4.0622	5.1435	28.0950
LP	35.1288	35.4172	67.1175
VA	6.9798	7.0181	25.2389
Our method	7.1719	7.0601	36.5388

We then test the methods’ robustness against complex clutters. Two shapes similar to the template shape but with different poses (the most similar one is indicated in red in the figure) are mixed together to generate the target point sets. Random outliers are then added to the target point sets. The aim is to animate complex clutter. We use the original SC distance measure in our method. Examples of shape matching by all the methods are shown in Fig. 4, It can be seen that, in addition to non-rigid deformation and random outliers, the mixing of similar shapes considerably complicates the matching problem. Despite the

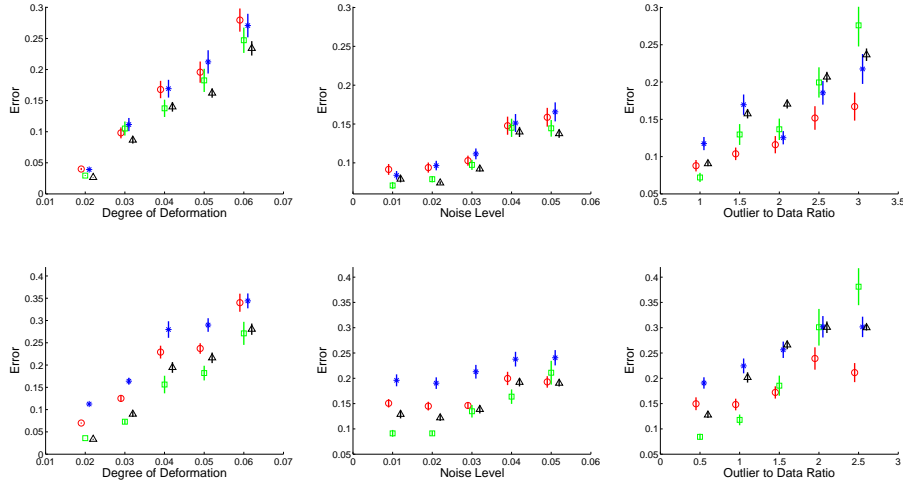


**Fig. 3.** Comparison of our method (red  $\circ$ ) with VA (green  $\square$ ), LP (blue  $*$ ) and LNRP (black  $\triangle$ ) on the Chui-Rangarajan synthesized data sets. The error bars indicate the standard deviation of the error over 100 random trials. Top row: fish tests. Bottom row: Chinese character tests.

difficulties, our method works much better at matching the template shapes to the correct target shapes than the other methods, validating the robustness of our method against complex clutters.

## 6.2 Experiments on real data

We finally test the methods' performance using data acquired from images. Examples of matching results by the competing methods are shown in Fig. 5, where the template shapes are further randomly rotated (not shown in the figure) with the aim at testing the methods' abilities for solving rotations. It can be seen that our method using ORSCD can successfully match to the correct shapes for all the tests, while our method using the original SC distance measure fails for the 3rd and 4th tests where similar shapes coexist in the same picture. This demonstrates ORSCD's robustness against structured outliers compared with the original SC distance measure. In comparison, LP fails for the 1st and 3rd tests, VA only succeeds for the 2nd test, and LNRP fails for all the tests. This clearly shows our method's potential for rotation invariant non-rigid shape matching arising from real problems.

## 7 Conclusion

We proposed a novel and efficient method for representing and matching non-rigid shapes. The representation is invariant to translational and rotational

changes, and by using a powerful feature descriptor and a new feature distance measure, it is also robust to non-rigid deformations and outliers. An algorithm was then proposed to solve the point matching problem, which possesses global optimality and is very robust against clutters. The proposed method was tested by using both simulated and real data in comparison with 3 state-of-the-art and representative methods. The results clearly demonstrated that the proposed method has high capability in detecting and matching shapes in cluttered scenes.

In the future, we will apply the proposed method to matching other types of rotation variant features such as local image patch and geometric blur.

## Acknowledgements

This research is supported by the Hong Kong RGC General Research Fund (PolyU 5351/08E) and the Hong Kong Polytechnic University Internal Fund (A-SA08).

## References

1. Chui, H., Rangarajan, A.: A new point matching algorithm for non-rigid registration. *Computer Vision and Image Understanding* **89** (2003) 114–141
2. Veltkamp, R.C., Hagedoorn, M.: State of the art in shape matching. (2001) 87–119
3. Besl, P.J., McKay, N.D.: A method for registration of 3-d shapes. *IEEE Trans. Pattern Analysis and Machine Intelligence* **14** (1992) 239–256
4. Zhang, Z.: Iterative point matching for registration of free-form curves and surfaces. *International Journal of Computer Vision* **13** (1994) 119–152
5. Stewart, C.V., Tsai, C.L., Roysam, B.: The dual-bootstrap iterative closest point algorithm with application to retinal image registration. *IEEE Trans. Medical Imaging* **22** (2003) 1379–1394
6. Fitzgibbon, A.W.: Robust registration of 2d and 3d point sets. *Image and Vision Computing* **21** (2003) 1145–1153 *British Machine Vision Computing 2001*.
7. Yuille, A.L., Kosowsky, J.J.: Statistical physics algorithms that converge. *Neural Comput.* **6** (1994) 341–356
8. Lian, W., Zhang, L., Liang, Y., Pan, Q.: A quadratic programming based cluster correspondence projection algorithm for fast point matching. *Computer Vision and Image Understanding* **114** (2010) 322–333
9. Sofka, M., Yang, G., Stewart, C.V.: Simultaneous covariance driven correspondence (cdc) and transformation estimation in the expectation maximization framework. In: *IEEE Conf. Computer Vision and Pattern Recognition*. (2007) 1–8
10. Tsin, Y., Kanade, T.: A correlation-based approach to robust point set registration. In: *European Conference on Computer Vision*. (2004) 558–569
11. Jian, B., Vemuri, B.C.: A robust algorithm for point set registration using mixture of gaussians. In: *IEEE International Conference on Computer Vision*. Volume 2. (2005) 1246–1251
12. Silva, L., Bellon, O.R., Boyer, K.L.: Precision range image registration using a robust surface interpenetration measure and enhanced genetic algorithms. *IEEE Trans. Pattern Analysis and Machine Intelligence* **27** (2005) 762–776

13. Sandhu, R., Dambreville, S., Tannenbaum, A.: Point set registration via particle filtering and stochastic dynamics. *IEEE Trans. Pattern Analysis and Machine Intelligence* **32** (2010) 1459–1473
14. Li, H., Shen, T., Huang, X.: Global optimization for alignment of generalized shapes. In: *IEEE Conf. Computer Vision and Pattern Recognition*. (2009) 856–863
15. Taylor, C.J., Bhusnurmath, A.: Solving image registration problems using interior point methods. In: *European Conference on Computer Vision*. (2008) 638–651
16. Jiang, H., Drew, M.S., Li, Z.N.: Matching by linear programming and successive convexification. *IEEE Trans. Pattern Analysis and Machine Intelligence* **29** (2007) 959–975
17. Jiang, H., Yu, S.X.: Linear solution to scale and rotation invariant object matching. In: *IEEE Conf. Computer Vision and Pattern Recognition*. (2009) 2474–2481
18. Kaick, O.v., Hamarneh, G., Zhang, H., Wightton, P.: Contour correspondence via ant colony optimization. In: *PG '07: Proceedings of the 15th Pacific Conference on Computer Graphics and Applications*. (2007) 271–280
19. Scott, C., Nowak, R.D.: Robust contour matching via the order-preserving assignment problem. *IEEE Trans. Image Processing* **15** (2006) 1831–1838
20. Wang, J., Athitsos, V., Sclaroff, S., Betke, M.: Detecting objects of variable shape structure with hidden state shape models. *IEEE Trans. Pattern Analysis and Machine Intelligence* **30** (2008) 477–492
21. Felzenszwalb, P.F.: Representation and detection of deformable shapes. *IEEE Trans. Pattern Analysis and Machine Intelligence* **27** (2005) 208–220
22. Coughlan, J.M., Ferreira, S.J.: Finding deformable shapes using loopy belief propagation. In: *European Conference on Computer Vision*. (2002) 453–468
23. Belongie, S., Malik, J., Puzicha, J.: Shape matching and object recognition using shape contexts. *IEEE Trans. Pattern Analysis and Machine Intelligence* **24** (2002) 509–522
24. Zheng, Y., Doermann, D.: Robust point matching for nonrigid shapes by preserving local neighborhood structures. *IEEE Trans. Pattern Analysis and Machine Intelligence* **28** (2006) 643–649
25. [http://en.wikipedia.org/wiki/Traveling\\_salesman\\_problem](http://en.wikipedia.org/wiki/Traveling_salesman_problem).
26. Thayananthan, A., Stenger, B., Torr, P.H.S., Cipolla, R.: Shape context and chamfer matching in cluttered scenes. In: *IEEE Conf. Computer Vision and Pattern Recognition*. Volume 1. (2003) 127–133

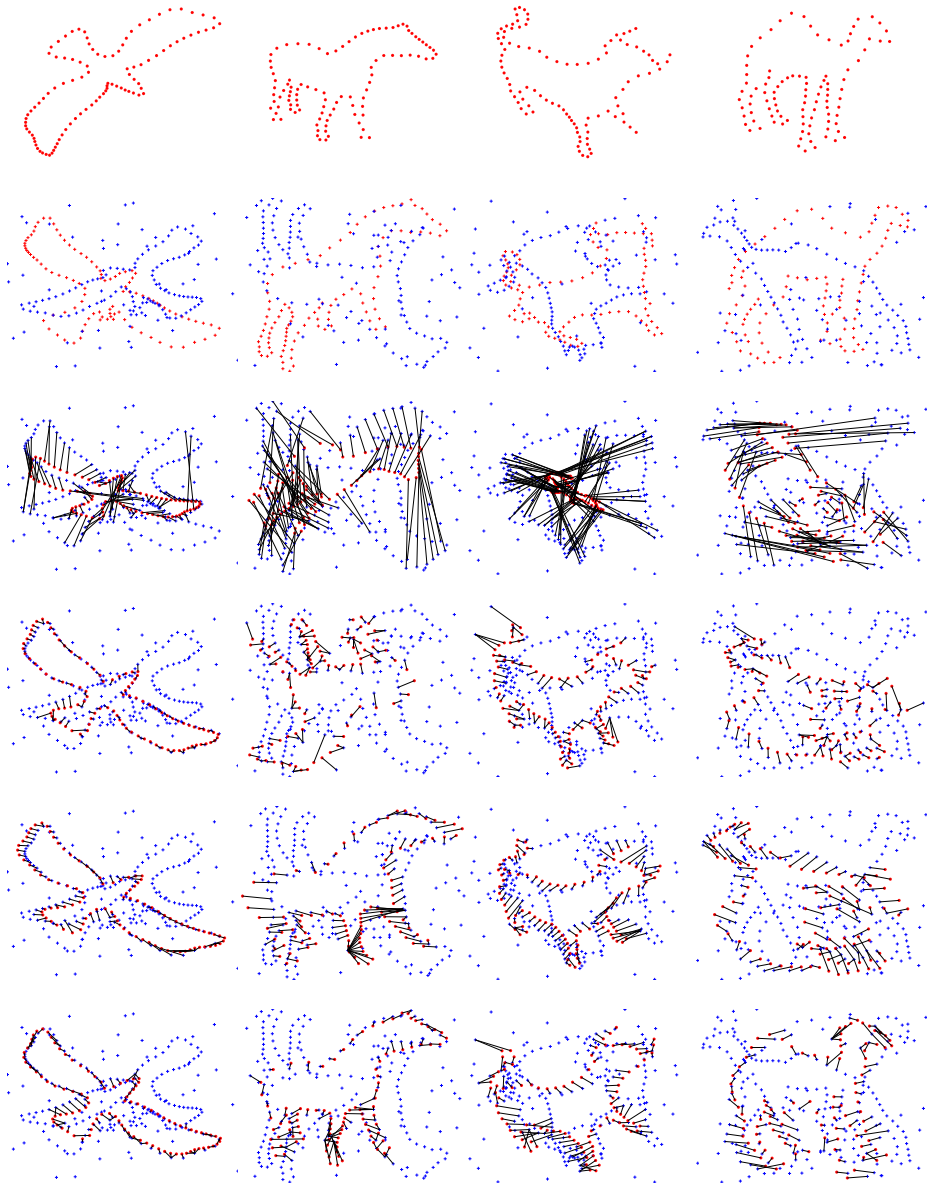


**Fig. 4.** Examples of point matching in case of complex clutter. The first row shows the template shapes. The second row shows the mixture of two shapes which are similar to the template shapes (the most similar ones are indicated in red) and random outliers. The last 4 rows show the matching results by LNSP, LP, VA and our method respectively.

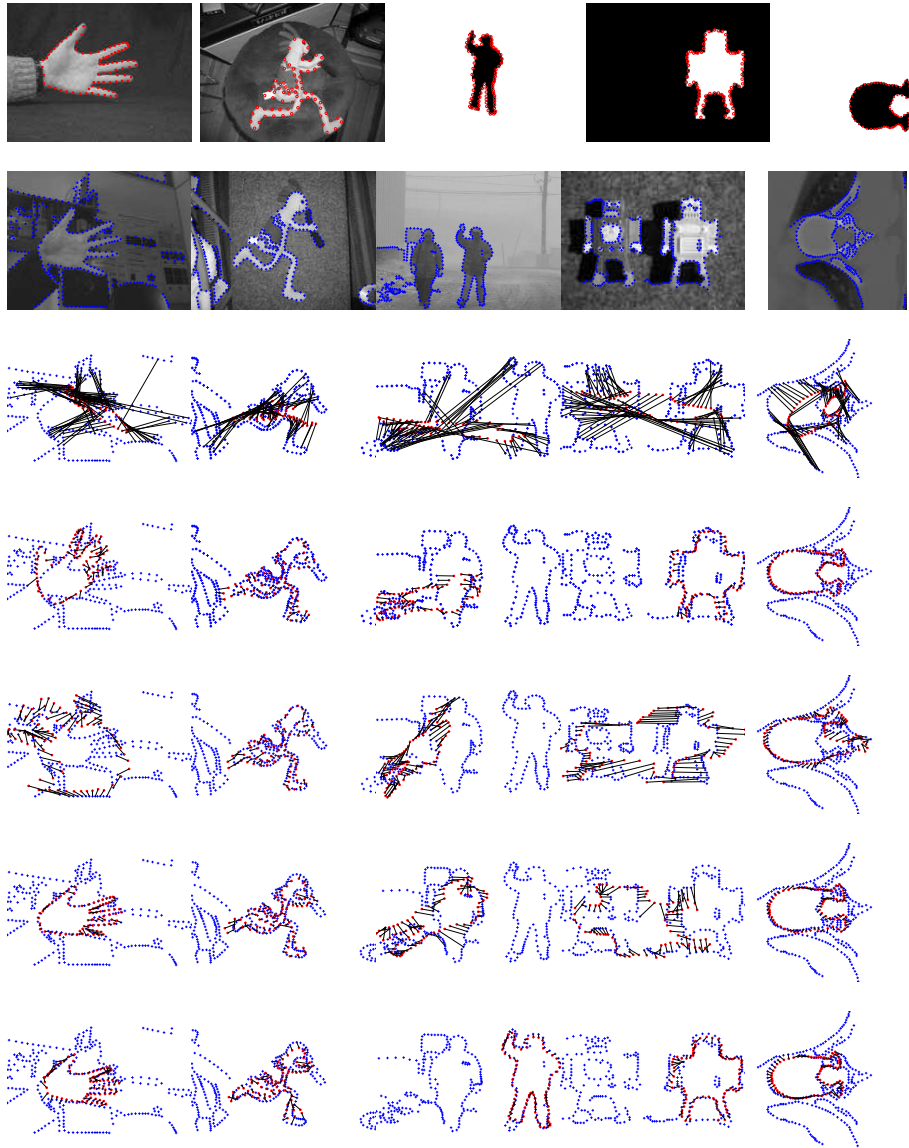


**Fig. 5.** Examples of point matching with data acquired from images. The first row shows the images used to extract the template point sets (red \*). The second row shows the images used to extract the target point sets (blue +). Points are extracted via Canny edge detector. The last 5 rows show the matching results by LNSP, LP, VA and our method using the original SC distance measure and ORSCD respectively.